Eur. Phys. J. D **8**, 443–449 (2000)

THE EUROPEAN PHYSICAL JOURNAL D

EDP Sciences

Efficient population transfer by delayed pulses despite coupling ambiguity

R. Unanyan[a], S. Guérin[b], B.W. Shore[c], and K. Bergmann

Fachbereich Physik, Universität Kaiserslautern, 67653 Kaiserslautern, Germany

Received 20 April 1999 and received in final form 15 July 1999

Abstract. In traditional schemes of multilevel multilaser excitation, each laser pulse interacts with only one pair of states, and the rotating wave approximation (RWA) is applicable. Here we study the population transfer process in a three-state system when each of the two lasers interacts with each of the pair of states and when the Rabi frequencies characterizing the interaction strengths of the system are comparable to or larger than the difference of the transition frequencies. We show that complete and robust population transfer is possible under conditions more general than those hitherto considered necessary for stimulated Raman adiabatic passage (STIRAP) or for successive π pulses. Using adiabatic Floquet theory we show that successful population transfer can be interpreted as adiabatic passage by means of a transfer state which connects the initial and final states. The Floquet picture offers a convenient interpretation of the population transfer as accompanied by multiple absorption of photons from or emission into the laser fields.

PACS. 42.50.Hz Strong-field excitation of optical transitions in quantum systems; multi-photon processes; dynamic Stark shift – 32.80.Wr Other multiphoton processes – 32.80.Bx Level crossing and optical pumping

1 Introduction

The time-varying population changes induced by two laser fields interacting with a three-state system exhibit a rich variety of phenomena and processes, such as lasing without inversion [1], laser cooling [2], population transfer [3], and loss-free pulse propagation [4,5] to name only a few. Most of the processes can be adequately treated within the limits imposed by the rotating wave approximation (RWA) [6]. One of the essential ingredients of this approximation is the requirement that each of the laser fields interacts only with one pair of levels, either because the difference of the transitions frequencies is sufficiently large or because optical selection rules (often related to laser polarization [7]) prevent additional couplings. In such cases the time evolution is dominated by two single-photon resonances, each associated with the exchange of a single photon between the laser fields and the atom or molecule.

In this article we generalize the well-known process of population transfer by stimulated Raman adiabatic passage (STIRAP [3]) to conditions beyond the validity of the RWA. The basic STIRAP process produces complete population transfer by means of two suitably delayed laser pulses: a pump pulse with carrier frequency $\omega_{\rm P}$ which couples the initial state $|1\rangle$ and an intermediate state $|2\rangle$, and a Stokes pulse with frequency $\omega_{\rm S}$ which couples the intermediate state to a final, target state $|3\rangle$, as diagrammed in Figure 1. For STIRAP, the pulses are applied in counterintuitive order: the Stokes pulse precedes the pump pulse. Complete population transfer from state $|1\rangle$ to state $|3\rangle$ is accompanied by the loss of a pump-field photon and the gain of a Stokes-field photon. We consider cases when the Rabi frequencies, although kept much smaller than the transition frequencies $\omega_{\rm P}$ and $\omega_{\rm S}$, as in the RWA, are comparable to or larger than the difference of the transition frequencies. No longer is there a clear identification of a particular pulse with a specific transition. Nevertheless, it is possible to achieve complete population transfer even under these conditions. We will see that multiple photon exchange becomes the mechanism of population transfer.

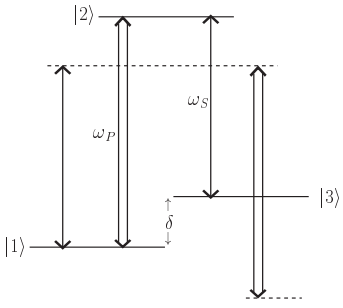

Fig. 1. Diagram of linkage patterns between three atomic states (full horizontal lines), showing pump (P) and Stokes (S) transitions.

[a] *Permanent address:* Inst. for Physical Research of Armenian Nat. Academy of Sciences, Ashtarak-2, 378410 Armenia.

[b] *Permanent address:* Laboratoire de Physique, CNRS, Université de Bourgogne, B.P. 47870, 21078 Dijon Cedex, France. e-mail: guerin@jupiter.u-bourgogne.fr

[c] *Permanent address:* Lawrence Livermore National Laboratory, Livermore, CA 94550, USA.

Several extensions of the conventional STIRAP theory beyond the RWA have been presented previously. The extensions include a discussion of population dynamics when the largest Rabi frequency approaches the difference of the transition frequencies [8], when the envelope of the laser pulses is not smooth but is modulated periodically [9] or when – in the extreme case – the Rabi frequency approaches the transition frequency [10].

The present work demonstrates that complete population transfer can result from pulse sequences that do not satisfy the usual conditions for counterintuitive pulses; in particular, both pulses act simultaneously on each transition. We show that in this regime the process is accompanied by degeneracies (or near-degeneracies) of dressed-state energies. These near-degeneracies have been previously observed for STIRAP with levels near the intermediate and final states [11,12] and for multiphoton $(2+1)$ STIRAP [10,13,14]. Such population transfer exhibits interesting effects of multiple-photon absorption from, or emission into, the laser fields. However, unlike the usual STIRAP, the transient population of the intermediate state is not negligible during the process. We examine the specific conditions leading to a robust population transfer, subjected to the approximation of a weakly lossy intermediate state. The extended regime for effective population transfer may apply when population transfer takes place between hyperfine states in atoms (see one example in [15]) or between states in groups of closely spaced levels in polyatomic molecules [16]. Alternatively, it becomes relevant when population transfer occurs in sufficiently strong laser fields, in the sense that the Rabi frequency approaches the space of the initial and final levels. (For example, this would require a peak field of order of 10^{15} W/cm^2 in a typical pulsed STIRAP experiment in NO [17].)

2 The Hamiltonian

The full Hamiltonian for the process reads

$$H(t) = H_0 + \mathbf{d}\cdot\mathbf{E}(t) \tag{1}$$

where H_0 is the Hamiltonian of the free three-level system, $\mathbf{d}$ the dipole moment operator (coupling transitions 1–2 and 2–3, but not 1–3) and $\mathbf{E}(t)$ the total electric field, expressed as

$$\mathbf{E}(t) = \mathbf{e}_\mathrm{S}\mathcal{E}_\mathrm{S}(t)\cos\omega_\mathrm{S}t + \mathbf{e}_\mathrm{P}\mathcal{E}_\mathrm{P}(t)\cos\omega_\mathrm{P}t, \tag{2}$$

and characterized by unit vectors $\mathbf{e}_j$ and real-valued functions of time $\mathcal{E}_j(t)$. The solution statevector $\Psi(t)$ of the system satisfies the time-dependent Schrödinger equation and the initial condition $|\Psi(-\infty)\rangle = |1\rangle$.

To parameterize the Hamiltonian matrix we introduce the usual time-dependent Rabi frequencies $\hbar\Omega_\mathrm{P}(t) = -\langle 1|\mathbf{d}\cdot\mathbf{e}_\mathrm{P}|2\rangle\mathcal{E}_\mathrm{P}(t)$ and $\hbar\Omega_\mathrm{S}(t) = -\langle 2|\mathbf{d}\cdot\mathbf{e}_\mathrm{S}|3\rangle\mathcal{E}_\mathrm{S}(t)$. We parameterize the ratio of the dipole moments as

$$\gamma \equiv \langle 1|\mathbf{d}\cdot\mathbf{e}_\mathrm{P}|2\rangle/\langle 2|\mathbf{d}\cdot\mathbf{e}_\mathrm{P}|3\rangle = \langle 1|\mathbf{d}\cdot\mathbf{e}_\mathrm{S}|2\rangle/\langle 2|\mathbf{d}\cdot\mathbf{e}_\mathrm{S}|3\rangle. \tag{3}$$

Another relevant parameter is the maximum Rabi frequency (maximized over time)

$$\Omega_\mathrm{max} = \max_t\{|\Omega_\mathrm{P}(t)|, |\gamma\Omega_\mathrm{S}(t)|, |\Omega_\mathrm{P}(t)/\gamma|, |\Omega_\mathrm{S}(t)|\}. \tag{4}$$

We consider, as is commonly done, the situation where the pump frequency ω_P is resonant with the 1–2 transition, and the Stokes frequency is resonant with the 2–3 transition,

$$\hbar\omega_\mathrm{P} = E_2 - E_1, \qquad \hbar\omega_\mathrm{S} = E_2 - E_3 \tag{5}$$

so that the pump-Stokes combination maintains the two-photon Raman resonance between initial state $|1\rangle$ and target state $|3\rangle$. A significant frequency is the beat frequency

$$\delta \equiv \omega_\mathrm{P} - \omega_\mathrm{S} = (E_3 - E_1)/\hbar. \tag{6}$$

We are interested in the transfer process when

$$|\delta| \lesssim \Omega_\mathrm{max}. \tag{7}$$

As is customary, we reduce the Schrödinger equation to three coupled ordinary differential equations and we eliminate the carrier frequencies by introducing the three-state rotating wave transformation [6],

$$\begin{aligned}\Psi(t) = {} & |1\rangle C_1(t) + |2\rangle C_2(t)\exp[-\mathrm{i}\omega_\mathrm{P}t] \\ & + |3\rangle C_3(t)\exp[-\mathrm{i}(\omega_\mathrm{P}-\omega_\mathrm{S})t].\end{aligned} \tag{8}$$

As with the RWA, we neglect terms that vary as sum frequencies. However, unlike the usual RWA, we retain terms that vary as the difference frequency δ. And, unlike the usual RWA, we do not assume that each of the two transitions is affected uniquely by a single pulse: we permit both pulses to act upon both transitions. In this sense, there is ambiguity of the couplings.

The resulting Hamiltonian $\hbar\mathsf{W}(t)$, for use with the equations

$$\mathrm{i}\frac{\mathrm{d}}{\mathrm{d}t}\mathbf{C}(t) = \mathsf{W}(t)\mathbf{C}(t) \tag{9}$$

has some elements that vary only with the pulse envelopes whereas other elements are modulated with the difference frequency δ

see equation (10) below.

$$\mathsf{W}(t) = \frac{1}{2}\begin{bmatrix} 0 & \Omega_\mathrm{P}(t) + \gamma\Omega_\mathrm{S}(t)\mathrm{e}^{-\mathrm{i}\delta t} & 0 \\ \Omega_\mathrm{P}(t) + \gamma\Omega_\mathrm{S}(t)\mathrm{e}^{+\mathrm{i}\delta t} & 0 & \Omega_\mathrm{S}(t) + [\Omega_\mathrm{P}(t)/\gamma]\,\mathrm{e}^{-\mathrm{i}\delta t} \\ 0 & \Omega_\mathrm{S}(t) + [\Omega_\mathrm{P}(t)/\gamma]\,\mathrm{e}^{+\mathrm{i}\delta t} & 0 \end{bmatrix} \tag{10}$$

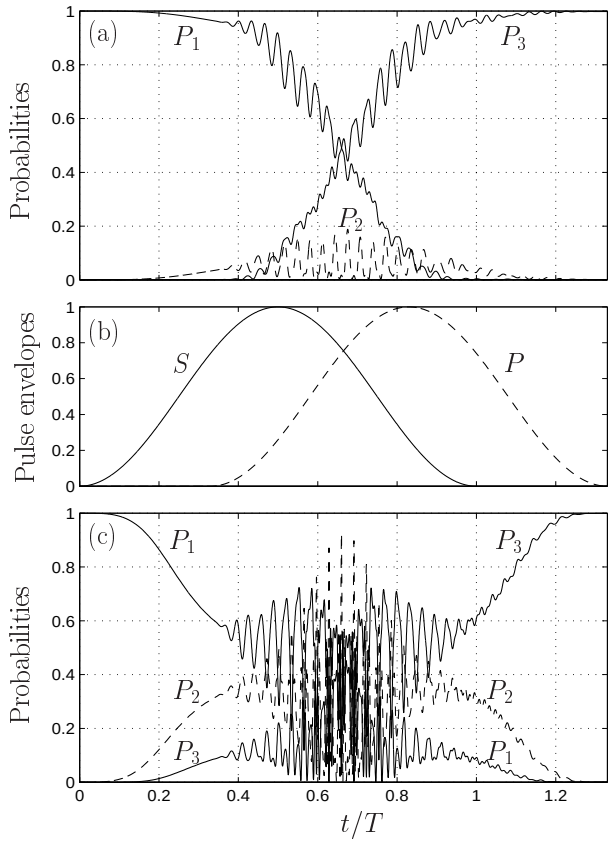

Fig. 2. Population histories $P_n(t)$ for $n = 1, 2, 3$, with $\delta = 2\Omega_0$, $\gamma = 1$, for (a) $\Omega_{\max} = \Omega_0$ (top frame), (c) $\Omega_{\max} = 4.4\Omega_0$ (bottom frame), and excitation by squared trig function pulse envelopes (of length $T = 100/\Omega_0$ and delay $0.33T$) with pump (dashed line) before Stokes (full line) shown in middle frame (b). Population transfer $P_3(\infty)$ to state $|3\rangle$ is nearly complete.

As is commonly done, we have assumed that spontaneous emission from the intermediate state $|2\rangle$ is negligibly small on the time scale of the pulse duration.

In the limit $\delta \to 0$, both transitions are driven by the same real-valued pulse. As with π-pulse processes, the degree of population exhibits an oscillatory dependence on the pulse area; it does not have the robust independence of pulse area which characterizes STIRAP.

When the beat frequency δ is much larger than either Rabi frequency, then one can drop terms involving $\exp[\pm i\delta]$, and the Hamiltonian reduces to the usual RWA description of STIRAP. Our interest here is in the alteration of the population dynamics when δ is not sufficiently large, and these terms must be retained.

3 Numerical results

In this section we present results obtained by numerically solving the time dependent Schrödinger equation (9), using the non-RWA Hamiltonian given in equation (10). These reveal some of the characteristic features of the influences of interaction parameters upon population dynamics. To ensure the interactions have a finite duration we use pulses based on the truncated $\sin^2$ envelope,

$$f(t) = \begin{cases} \sin^2(\pi t/T) & 0 < t < T, \\ 0 & \text{otherwise.} \end{cases} \tag{11}$$

Time and frequency are scaled to a Rabi frequency Ω_0. In this paper we set the scaled pulse length to $T = 100/\Omega_0$. Thus, if the relevant Rabi frequencies Ω are sufficiently large to satisfy $\Omega/\Omega_0 > 0.1$, the standard STIRAP condition for adiabatic evolution [3] is fulfilled. As with conventional STIRAP, we look for conditions which will produce complete population transfer into target state $|3\rangle$. For simplicity we take the two pulses to have equal peak values, and $\gamma = 1$. Thus for fixed pulse delay the computations presented here involve only two parameters, the peak Rabi frequency $\Omega_{\max}$ and the beat frequency δ.

3.1 Evolution of the population

Figure 2 shows two examples of successful population transfer. The upper and lower frames of Figure 2 show the time varying populations of the three atomic states for two choices of peak Rabi frequency, $\Omega_{\max} = \Omega_0$ and $4.4\Omega_0$, respectively. The middle frame shows the pulses, of the form (11), used for the calculation (parameters are given in the caption). With these parameters of the pulses the standard condition [3] for adiabatic evolution is fulfilled.

For $\Omega_{\max} = \Omega_0$ (upper frame), the peak Rabi frequency is smaller than δ. This situation is similar to standard STIRAP, and complete population transfer occurs. Because we have not applied the usual RWA, the evolution $P_n(t)$ is not smooth. The oscillations are a first correction of the usual RWA-based STIRAP, as studied in [8].

For $\Omega_{\max} = 4.4\Omega_0$ (lower frame), the peak Rabi frequency is larger than the difference of the transition frequencies, and so the conditions for conventional STIRAP do not apply. Nevertheless, complete population transfer occurs. However, although conditions fulfill the usual adiabaticity criterion of STIRAP, unlike STIRAP there occurs substantial transient population in the intermediate state $|2\rangle$. Furthermore, the amplitude of the oscillations of $P_n(t)$ are substantially larger than for $\Omega_{\max} = \Omega_0$.

As these examples show, it is possible to achieve good population transfer even though the effective Hamiltonian embodies modulations that one might expect to hinder such transfer, and although the pulses are not uniquely interacting with a single transition. It is natural to ask whether such transfer is robust to small changes of Rabi frequency, as is traditional STIRAP, or whether the transfer exhibits the periodic dependence on pulse area characteristic of multiple-π pulses.

3.2 Dependence on Rabi frequency and detuning

The answer to the question posed at the end of the previous paragraph is found by inspection of Figure 3, which

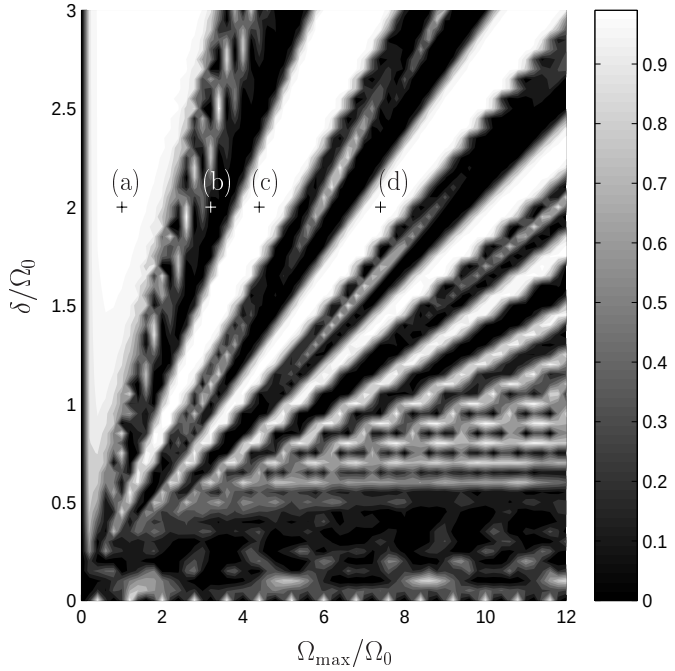

Fig. 3. Contour map of population transfer efficiency $P_3(\infty)$ for varying difference frequency δ and varying peak Rabi frequency $\Omega_{\max}$ (the other parameters are the same as in Fig. 2). The crosses (all along the line $\delta = 2\Omega_0$) labelled (a) ($\Omega_{\max} = \Omega_0$) and (c) ($\Omega_{\max} = 4.4\Omega_0$) refer to the parameters of the simulations of Figures 2a and 2c, respectively. The crosses also refer to the parameters relevant for Figures 6a and 6b ($\Omega_{\max} = 3.2\Omega_0$), 6c and 6d ($\Omega_{\max} = 7.4\Omega_0$), respectively.

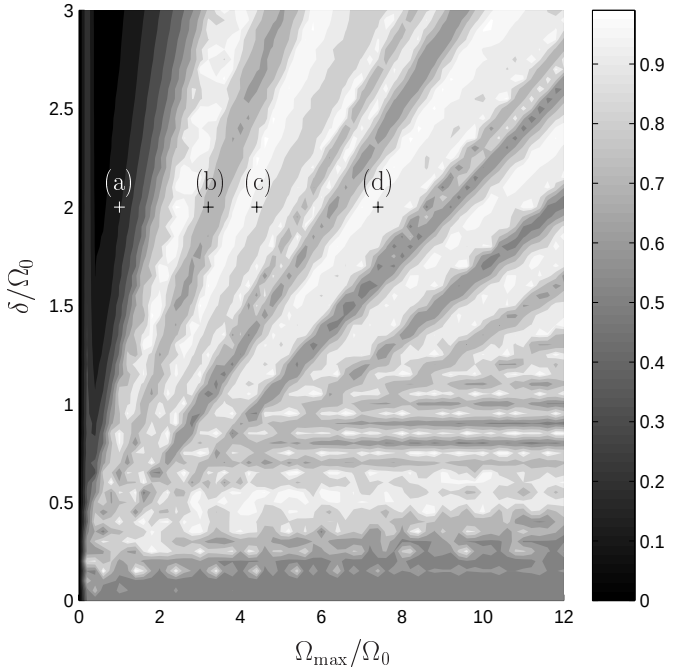

Fig. 4. Maximum instantaneous population in state $|2\rangle$ during the pulses, P_{trans}, as a function of peak Rabi frequency and δ.

shows the variation of the transfer efficiency $P_3(\infty)$ with δ and $\Omega_{\max}$.

The lower horizontal portion of the figure shows a complicated partially-regular pattern with isolated regions of high (white) and low (black) transfer efficiency. The upper portion, on the other hand, shows a more regular pattern: a succession of ridges of high transfer efficiency and valleys of low transfer efficiency. The ridges and valleys extend radially from the origin. The two crosses (a) and (c) identify the combination of parameters used for the calculations shown in Figure 2.

The white ridge adjacent to the vertical axis marks the region of the standard STIRAP process ($\delta \gg \Omega_{\max}$). The well-known robustness of the STIRAP transfer efficiency with respect to a variation of the Rabi frequency is seen here as white region which grows wider as δ increases. The STIRAP population transfer is observed, wherever the peak Rabi frequency is large enough to satisfy the adiabatic criterion (see also left part of Fig. 4). In addition to this region of high transfer efficiency, there is a succession of regions of equally high efficiency, with successively narrower widths (and hence successively less robustness). Unlike the standard STIRAP ridge, the high population transfer of these additional ridges is accompanied by substantial transient population in the intermediate level (see also the lower frame of Fig. 2) which decreases for larger peak Rabi frequency $\Omega_{\max}$.

3.3 Transient population in the intermediate level

The standard STIRAP procedure accomplishes nearly complete population transfer while placing negligible population into the intermediate state $|2\rangle$. This property is useful to avoid population loss through spontaneous emission from that state. To show how an increase of Rabi frequency affects this population, Figure 4 shows the value of the maximum transient population in state $|2\rangle$, P_{trans}, as a function of δ and the peak Rabi frequency.

We recognize the dark nearly-vertical valley (black), coincident with the ridge (white) of Figure 2 where standard STIRAP takes place. We also note here the same pattern of radial ridges and valleys as in Figure 2; there are regimes in which nearly all population resides momentarily in state $|2\rangle$. Except in the STIRAP region, no structures appear clearly on this diagram, which would allow low transient population (say less than 30%) of the intermediate state with high transfer.

3.4 Changing the degree of coupling ambiguity

When γ deviates from unity, the symmetry of the couplings is broken and population transfer is less efficient. As an example, Figure 5 shows the variation of the slope and the width of the ridges (white, high transfer) and the valleys (dark, low transfer) for $\gamma = 0.8$, as compared to $\gamma = 1$. The structure adjacent to the STIRAP zone almost disappears for $\gamma = 0.7$ (not shown).

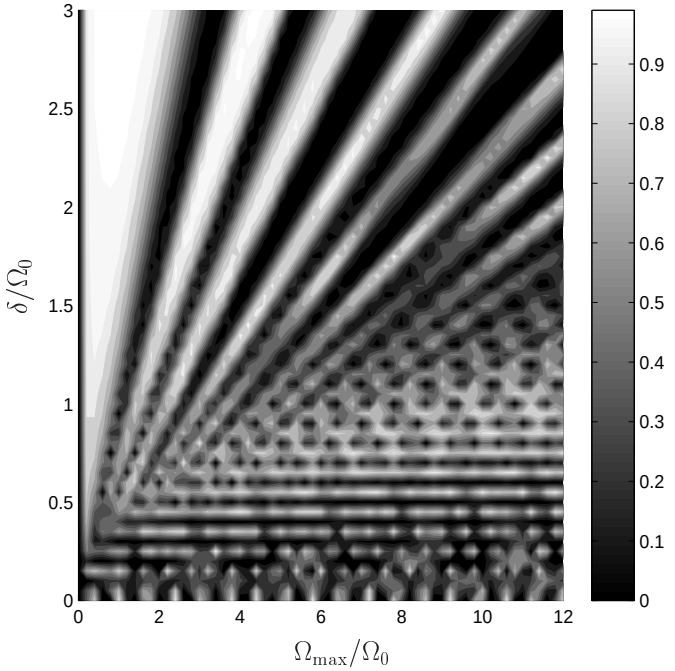

Fig. 5. Contour map of population transfer efficiency $P_3(\infty)$ for $\gamma = 0.8$ (the other parameters are the same as in Fig. 2).

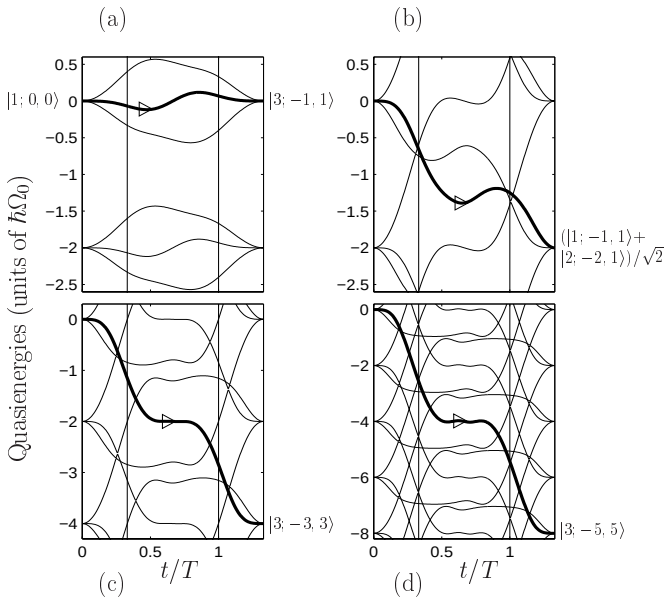

Fig. 6. Four frames of Floquet eigenvalues with $\delta = 2\Omega_0$, $\gamma = 1$, for (a) $\Omega_{\max} = \Omega_0$, (b) $\Omega_{\max} = 3.2\Omega_0$, (c) $\Omega_{\max} = 4.4\Omega_0$, and (d) $\Omega_{\max} = 7.4\Omega_0$. Other conditions are as in Figure 2. The parameters used to calculate the curves are marked in Figure 3. Vertical lines indicate where respectively (from left to right) pump starts and Stokes ends.

4 Interpretation using adiabatic Floquet theory

In this section we use adiabatic Floquet theory to offer an explanation for the patterns of high and low transfer efficiency presented above. The mean carrier frequencies have already been removed from the Hamiltonian (10). If we disregard the slow variation of the pulse envelopes we are left with a Hamiltonian whose elements vary periodically with the frequency δ – conditions which allow the use of Floquet theory and assure that we can express the statevector as a linear combination of the eigenstates of the Floquet Hamiltonian [18–20].

In the processes to be discussed here, the amplitudes of the laser fields are not constant. Therefore we are not dealing with a strictly periodic Hamiltonian. Nevertheless, the essential physics can be discussed based on the Floquet approach.

When the interaction energies (the Rabi frequencies) are negligibly small, and the carrier frequencies are tuned to resonance with their respective transition frequency (as we assume), the spectrum of the Floquet Hamiltonian consists of a ladder of equally-spaced triply-degenerate eigenvalues. The spacing is given by the characteristic frequency, which is here δ. The degeneracy is removed during the course of the interaction, whenever the Rabi frequencies are non-zero. The related eigenstates are characterized by $|n; n_{\rm P}, n_{\rm S}\rangle$, where $n = 1$, 2 or 3 identifies the atomic state and $n_{\rm P}$ or $n_{\rm S}$ are the incremental photon numbers in the pump or Stokes radiation field, respectively. The reference state $|1;0,0\rangle$ describes the system with the atom in its ground state $|1\rangle$ before photons are absorbed or emitted. After a standard STIRAP process, with absorption of one photon from the pump field and emission of one photon into the Stokes field, the system is described by $|3;-1,+1\rangle$. The eigenstates whose energies border the energy of the state $|1;0,0\rangle$ are $|1;N,-N\rangle$, with N a negative or positive integer. If δ and N are positive, then the energy of state $|1;N,-N\rangle$ lies above that of state $|1;0,0\rangle$.

Figure 6 presents examples of the time-dependent adiabatic Floquet eigenvalues (or quasienergies) for four values of the peak Rabi frequency. In each frame a pair of vertical lines bound the time interval when both pulses are present: to the left of the lines only the Stokes pulse acts, to the right only the pump pulse is present.

At very early and very late times, when all Rabi frequencies are negligibly small, the energies of the groups of triply degenerate states are well-separated (by a positive or negative integer number of increments of the frequency δ). At intermediate times, the degeneracy is removed and the separation between the lowest eigenvalue of a given triplet and the highest eigenvalue of the neighboring lower triplet is reduced. In frame (a), the triplet of Floquet eigenvalues always form a distinct set. In subsequent frames Floquet manifolds overlap.

The system starts in state $|1;0,0\rangle$. We define the *transfer state* to be the particular eigenstate of the adiabatic Floquet Hamiltonian which evolves from this state. The population resides in the transfer state [21,22,14]. The evolution of the eigenenergies of this state is shown in Figure 6 as a thick line.

As the energy evolves, the transfer-state eigenvalue may reach regions of avoided crossings. Adiabatic passage through such a region is one key to the successfull completion of population transfer since it is associated with

transitions between atomic basis states [21,22]. Thus when the evolution is adiabatic the population remains in one and only one Floquet eigenstate. Diabatic evolution of the transfer state may occur through some real or sufficiently weakly avoided crossings. During such diabatic evolution, the transfer state jumps from one Floquet eigenstate to another. As described in an example below, the key to successfull population transfer is a combination of the overall adiabatic evolution with some localized diabatic process. This combination allows in specific conditions the transfer state to connect the initial dressed state $|1;0,0\rangle$ with the final atomic state combined with any number of photons N such as $|3;-N,N\rangle$ [14,22].

Figure 6a gives an example of a standard STIRAP process (the history shown in Fig. 2a) for transfer between state $|1\rangle$ and $|3\rangle$ with the exchange of one photon per radiation field, *i.e.* $|1;0,0\rangle \longrightarrow |3;-1,1\rangle$. The population evolves along the path which stays close to zero energy. The small deviation of the transfer path from zero energy means that the intermediate-state population remains small [10].

The path of the transfer-state eigenvalue for a larger Rabi frequency is shown in Figure 6b, with parameters which place the system in a location close to the bottom of a valley (low transfer) of Figure 3. Here the energies of neighboring groups of triplets cross. When this happens the dynamics is more complicated (and more interesting). In the case shown, the transfer path follows, at late times, the upper curve of the lower triplet. This implies that adiabatic evolution is not into the final state $|3\rangle$ but into a superposition of initial and intermediate state: $(1/\sqrt{2})(|1;-1,1\rangle + |2;-2,1\rangle)$. Such a superposition state is characteristic for the situation discussed here. When $\delta \gg \Omega_{\max}$, as in standard STIRAP, the absorption and emission process brings the population into the target state $|3\rangle$. However, when $\delta \lesssim \Omega_{\max}$, the population may also return to states $|1\rangle$ and $|2\rangle$.

To understand the dynamics we examine the time evolution of the transfer-state eigenvalue at each instant. For instance, we analyse the one of frame (b) of Figure 6. First it meets a crossing which is real (because only one laser is acting). Next it encounters a crossing which is avoided but very weak, because it occurs very close to the beginning of the pump pulse when the coupling is weak between the two states involved. The diabatic approximation can be made here for both these crossings: the transfer-state eigenvalue crosses them diabatically. (Because $\gamma = 1$ the same argument applies equivalently near the end of the process.) Next, between the beginning of the pump pulse and the end of the Stokes laser (where no real crossing are allowed), the transfer-state eigenvalue meets avoided crossings. Since here the transfer-state eigenvalue connects $|1\rangle$ with $(1/\sqrt{2})(|1;-1,1\rangle + |2;-2,1\rangle)$, a robust superposition of states $|1\rangle$ and $|2\rangle$ is formed. The transfer fails. Equivalent arguments about the occurrence of crossings or avoided crossings apply for the other eigenvalues shown in the other frames.

Frames (c) and (d) of Figure 6 show cases of successful population transfer with successively larger values of peak Rabi frequency. These represent, respectively, the transfer of three and five photons with each radiation field (*i.e.* transfer from $|1;0,0\rangle$ to $|3;-3,3\rangle$ or $|3;-5,5\rangle$, for frames (c) or (d), respectively). Multiple photon up-down-up processes have been discussed in two-level systems, for instance, by Reuss and coworkers [23].

From the discussion above, and by inspection of Figures 3 and 6, it is apparent that there exist an infinite sequence of ridges and valleys (Fig. 3), each associated with parameters that maximize or minimize population transfer from state $|1\rangle$ to state $|3\rangle$. The ridge closest to the vertical axis identifies the standard STIRAP region. In this region $\delta \gg \Omega_{\max}$ is valid and γ has few if any consequences. Each radiation field exchanges one photon with the atom or molecule. Along the neighboring ridges population transfer from $|1\rangle$ to $|3\rangle$ involves the exchange of 3, 5, ... $2N+1$ ... photons (of each field), leading to states which are to be characterized as $|3;-1-2N,1+2N\rangle$ (with N a positive integer). The occurrence of these photon numbers can be qualitatively understood by considering the three-state system as two independent two-state systems: for moderate intensities two-state systems can absorb or emit only odd number of one-photon resonant photons [18].

The transient population in the intermediate state $|2\rangle$ is only small in the region of the first ridge. When the parameters place to system in one of the valley-regions (Fig. 3), the system remains in a superposition state characterized as $(|1;-(2N+1),2N+1\rangle + |2;-2(1+N), 2N+1\rangle)/\sqrt{2}$.

5 Conclusions

We have examined the process of stimulated Raman adiabatic passage (STIRAP) for the case that a peak Rabi frequency is larger than the difference between the two carrier frequencies, so that both radiation fields can interact with each transition dipole moment – the one between the initial and the intermediate state as well as the one between the intermediate and final state. We have shown that complete robust population transfer is possible under certain conditions with the exchange of one or more (odd number) of photons between each radiation field and the atom or molecules. When the transfer process is associated with the exchange of more than one photon per radiation field, the transient population of the intermediate level is no longer negligibly small, even when the evolution is adiabatic.

Observation of the transfer scenarios discussed here is not restricted to the use of high power lasers. Since the relevant parameter is δ/Ω, any system with nearly degenerate states could be used as an example. The energy separation of the states could, for instance, be controlled by a magnetic field, as was already done in connection with the STIRAP process implemented for Ne^* atoms in their metastable states [7,12]. Helium is a particularly interesting system, because of its relatively long lived excited states, which can be reached from the (intermediate)

metastable state $^3S_1$ by radiation in the near infrared, visible or ultraviolet region of the spectrum. Some interesting consequences of the multiphoton transfer process to momentum transfer and the deflection of particles will be the subject of a related publication [24].

RU and SG thank H.R. Jauslin, M. Fleischhauer and N.V. Vitanov for useful discussions. RU thanks the Alexander von Humboldt-Stiftung for a Fellowship. SG thanks "La Fondation Carnot" for support. BWS thanks the Alexander von Humboldt-Stiftung for a Research Award; the work of BWS is supported in part under the auspices of the U.S. Department of Energy at Lawrence Livermore National Laboratory under contract W-7405-Eng-48. This work was supported by the European Union HCM network ERB-CHR-XCT-94-0603 and by the Deutsche Forschungsgemeinschaft.

References

1. M.O. Scully, Phys. Rep. **219**, 191 (1992).
2. S. Chu, Rev. Mod. Phys. **70**, 685 (1998); C. Cohen-Tannoudji, Rev. Mod. Phys. **70**, 707 (1998); W.D. Phillips, Rev. Mod. Phys. **70**, 721 (1998).
3. U. Gaubatz, P. Rudecki, S. Schiemann, K. Bergmann, J. Chem. Phys. **92**, 5363 (1990); K. Bergmann, H. Theuer, B.W. Shore, Rev. Mod. Phys. **70**, 1003 (1998).
4. S.E. Harris, Phys. Rev. Lett. **72**, 52 (1994),
5. M.D. Lukin, M. Fleischhauer, A.S. Zibrov, H. Robinson, V.L. Velichansky, L. Hollberg, M.O. Scully, Phys. Rev. Lett. **79**, 2959 (1997).
6. B.W. Shore, *The Theory of Coherent Atomic Excitation* (Wiley, New York, 1990).
7. H. Theuer, K. Bergmann, Eur. Phys. J. D **2**, 279 (1998).
8. S. Guérin, R.G. Unanyan, L.P. Yatsenko, H.R. Jauslin, Opt. Expr. **4**, 84 (1999).
9. L.P. Yatsenko, B.W. Shore, K. Bergmann, V.I. Romanenko, Eur. Phys. J. D **4**, 47 (1998).
10. S. Guérin, H.R. Jauslin, Eur. Phys. J. D **2**, 99 (1998).
11. B.W. Shore, J. Martin, M.P. Fewell, K. Bergmann, Phys. Rev. A **52**, 566 (1995); J. Martin, B.W. Shore, K. Bergmann, Phys. Rev. A **52**, 583 (1995).
12. J. Martin, B.W. Shore, K. Bergmann, Phys. Rev. A **54**, 1556 (1996).
13. L.P. Yatsenko, S. Guérin, T. Halfmann, K. Böhmer, B.W. Shore, K. Bergmann, Phys. Rev. A **58**, 4683 (1998).
14. S. Guérin, L.P. Yatsenko, T. Halfmann, B.W. Shore, K. Bergmann, Phys. Rev. A **58**, 4691 (1998).
15. S. Menon, G.S. Agarwal, Phys. Rev. A **59**, 740 (1999).
16. G. Herzberg, *Molecular spectra and molecular structure I. Spectra of diatomic molecules* (D. van Nostrand Company, Inc., Toronto, 1963).
17. S. Schiemann, A. Kuhn, S. Steuerwald, K. Bergmann, Phys. Rev. Lett. **71**, 3637 (1993).
18. J.H. Shirley, Phys. Rev. B **138**, 979 (1965).
19. Ya.B. Zeldovich, JETP **24**, 1006 (1967).
20. S. Guérin, F. Monti, J.M. Dupont, H.R. Jauslin, J. Phys. A **30**, 7193 (1997).
21. H.P. Breuer, M. Holthaus, Phys. Lett. A **140**, 507 (1989); M. Holthaus, Phys. Rev. Lett. **69**, 1596 (1992); S. Guérin, H.R. Jauslin, Phys. Rev. A **55**, 1262 (1997).
22. S. Guérin, Phys. Rev. A **56**, 1458 (1997).
23. M. van Opbergen, N. Dam, A.F. Linskens, J. Reuss, B. Sartakov, J. Chem. Phys. **104**, 3438 (1996)
24. L. Yatsenko (personal communication, 1998).